Turbulence signatures in high–latitude ionospheric scintillation

K. Meziane[1], A. M. Hamza[1], and P. T. Jayachandran[1]

[1]Physics Department, University of New Brunswick, Fredericton, Canada.

Key Points:

- Evidence for the existence of a linear range in the the structure function of ionospheric scintillation
- The structure function slope in the linear range is consistent with the scaling exponent of the ionospheric electron density fluctuations
- Indications that the equilibrium state related to scintillation is dominated by non-Gaussian statistics

Corresponding author: K. Meziane, karim@unb.ca

Abstract

Ground-based amplitude measurements of GNSS signal during ionospheric scintillation are analyzed using prevalent data analysis tools developed in the fields of fluid and plasma turbulence. One such tool is the structure function of order q, with $q = 1$ to $q = 6$, which reduces to the computation of the second order difference in the GPS signal amplitude at various time lags, and allows for the exploration of dominant length scales in the propagation medium. We report the existence of a range where the structure function is linear with respect to time lag. This linear time-segment could be considered as an analog to the inertial range in the context of neutral and plasma turbulence theory. Below the linear range, the structure function increases nonlinearly with time lag, again in good concordance with the intermittent character of the signal, given that a parallel is drawn with turbulence theory. Quantitatively, the slope of the structure function in the linear range is in good agreement with the scaling exponent determined from in-situ measurements of the electrostatic potential at low altitude (E-region) and the electron density at the topside ionosphere (F-Region). This in turn suggests the conjecture that scintillation could be considered a proxy for ionospheric turbulence. Furthermore, we have found that the probability distribution function of the second order difference in the signal amplitude has non-Gaussian features at large time-lags; a result that seems inconsistent with equilibrium statistical physics which suggests a Gaussian distribution for the conventional random walk processes.

1 Introduction

Ionospheric scintillation is the physical phenomenon associated with distortions that arise in Global Navigation Satellite System (GNSS) radio wave fronts as they propagate through the ionosphere (Kintner et al., 2001). It is imputable to irregularities in ionospheric electron density, which arise from various plasma instabilities. As a consequence, structures in electron density form, which in turn affect the dielectric properties of the medium including its refractive index. Radio waves propagating through a structured ionosphere are scattered, and it is the signatures of various scattering processes that allow us to extract some of the fundamental ionospheric properties without in-situ measurements, a reverse engineering exercise. On the ground, a GNSS receiver records a time-series and reveals patterns which very much depend on the spatial and temporal conditions of the ionospheric medium through which the radio signal propagated. In other words, we ought to be able, through the principle of Inverse Scattering, to reconstruct some of the physical properties of the scattering medium. The scintillations recorded by the GNSS receiver hold integrated information about the ionospheric irregularities, their temporal and spatial scales, which can help narrow down the ionospheric plasma instability mechanisms at play. As an example, the equatorial anomaly (Groves et al., 1997) has long been understood as the cause of scintillation near the geomagnetic equator. In the ionospheric E and F regions, plasma instabilities such as the Farley-Buneman (Hamza & St-Maurice, 1993) and the gradient-drift are believed to be two of the most fundamental driving mechanisms that give rise to plasma density irregularities with characteristic length scales ranging from few centimetres to hundreds of kilometres (Aarons, 1982; Yeh & Liu, 1982; Wernik et al., 2007; Kintner et al., 2007). The size of these irregularities plays a central role when analyzing and especially when interpreting the data, which requires the knowledge to differentiate between refractive and diffractive signatures. Identifying the Fresnel field region and testing the Taylor frozen hypothesis to derive a temporal scale from the Fresnel scale are two of the most important steps in the interpretation of scattering data recorded by the GNSS receiver.

Empirically, scintillation studies use observables measured by GNSS receivers. Both signal's amplitude and phase are derived from the recorded measurements. For as long as lock is maintained between the satellite and the ground receiver, continuous measurements of the amplitude and phase can be recorded at usually a very high rate. When

the ray path (between the satellite orbiting at $\sim 20,000$ km from the centre of Earth) interacts with ionospheric irregularities, enhanced fluctuations rising above the background level in the signal's phase and amplitude appear. The conventional approach is to quantify the signal fluctuations using the scintillation indices S_4 and σ_Φ indices corresponding to the variance of the amplitude and phase variations, respectively.

The theoretical investigation of scintillation uses the wave equation as formulated for a random medium. An analytical closed form solution for the general case is not available as the equation contains a stochastic parameter directly related to the density of scatterers. Approximations based on the nature of the interaction of the radio signal with the medium have been considered by several authors in order to derive the signal's electric field. These models include the weak-scattering theory, the Rytov approximation and the phase screen theory based on a thin conducting layer approximation (Yeh & Liu, 1982; Priyadarshi, 2015). Under these models, ionospheric irregularity power spectra combined with the wave equation provide elements of comparison between theory and observations.

In the present work, tools developed in the context of neutral fluid and plasma turbulence theories are used in order to unveil pertinent and dominant length scales responsible for ionospheric scintillation. This path has been initiated in a previous report in which intermittency was explored in ionospheric scintillation (Mezaoui et al., 2015); a statistical mechanics' approach, which analyzes the properties of fluctuations of the local variable measured, was used. These fluctuations tend to deviate from the homogeneous and isotropic model of turbulence introduced by Taylor (1935, 1938), and have consistently been labeled as intermittent. This approach may be justified given that various physical mechanisms can lead the ionospheric plasma to a turbulent state, particularly when plasma instabilities evolve toward a nonlinear regime. Ionospheric plasma turbulence, driven by various instability mechanisms, which give rise to density irregularities, often exhibit an electron density power spectrum with a power law qualitatively similar to the Kolmogorov (1941) power law for the velocity field in the context of fluid turbulence theory. The mathematical framework used in the present work is briefly depicted in Section 2, while Section 3 describes the data. In Section 4, the results are presented followed by a discussion section (Section 5).

2 The Structure Function

The fields of neutral fluid and plasma turbulence are mature research fields that have evolved for more than a century. A number of mathematical tools have been developed to quantify and capture the underlying physical mechanisms responsible for the turbulent structure of the neutral fluid or the plasma, respectively. The statistical mechanics approach consists of estimating ensemble properties that can be derived by coarse-graining the fields and studying the dependence of the fluctuations on the coarse-graining scales. This has led fluid dynamicists, for example, to study the probability distribution of the velocity increment $U(r+\delta) - U(r)$ instead of solving the Navier-Stokes equation (Benzi et al., 1993), a nonlinear partial differential equation with no closed form solutions known in the case of turbulence; the probability distribution is then found to be skewed. Skewness would vanish only if there were invariance under time reversal, but for a turbulent dissipative flow this is not the case (for a mathematical proof, see (Lawrance, 1991; Sosa-Correa et al., 2019)). This result has profound consequences since one is often led to believe that the probability distributions ought to be normal or log-normal, which would imply a zero skewness, a result that is inconsistent with observations. As stated by the Nobel Prize laureate David Ruelle, "the lognormal theory contains an element of truth but has limited applicability" (https://arxiv.org/abs/1405.5746).

To illustrate the use of this statistical approach, we focus on the coarse-grained one-dimensional velocity fluctuations. One is then able to extend the method to the case of

plasma fluctuations, including the flow velocity fluctuations, the electric and magnetic field fluctuations or a combination. In this context, and in the fluid flow velocity $U(r)$ case, the structure function of order q is defined as follows (Chang, 2015):

$$D_q(\delta) = \left\langle \, |U(r+\delta) - U(r)|^q \, \right\rangle \tag{1}$$

where $\left\langle \right\rangle$ represents the ensemble average. In Expression (1), the difference of the flow speed U is between two points spatially separated by the scale δ. For simplicity, the structure function $D_q(\delta)$ is formulated in the one dimensional case. The conventional analysis consists of exploring the dependence of the structure function on the coarse-graining scale δ and the exponent index q. A turbulent system with a Kolmogorov scaling is consistent with a structure function in the form:

$$D_q(\delta) \sim \delta^{\xi(q)} \tag{2}$$

Within the inertial range, where the equilibrium state is characterized by self-similarity and the power spectrum by a power law, the structure function $D_q(\delta)$ is supposed to remain linear in δ independent of q. For the particular case of Kolmogorov turbulence, $\xi(q) = q/3$; in other words, the structure function of order 3 is $S_3 \sim \delta$. It is worth elaborating on the Kolmogorov result, which is based on the suggestion by Obukov (1962) that the average rate of energy dissipation per unit mass $\langle \epsilon \rangle$ should be replaced by the spatially averaged dissipation defines as:

$$\epsilon_\delta = \frac{1}{\delta} \int_{r_0}^{r_0+\delta} \epsilon(r) dr \tag{3}$$

Kolmogorov (1962) introduced a refined self-similarity hypothesis relating the structure functions for the flow velocity to the moments of the scale dependent rate of energy dissipation.

$$D_q(\delta) = C_q \langle (\epsilon)^{\frac{q}{3}} \rangle \delta^{\frac{q}{3}} \tag{4}$$

The essential result of this hypothesis is that the statistics of $S_3(\delta)/\delta$ is the same as the statistics of ϵ_δ. In other words, the ratio $S_3(\delta)/\delta\epsilon_\delta$ is a random variable with a universal distribution. A similar argument can be extended to higher order structure function by noting that $D_q(\delta) \sim D_3(\delta)^{\xi(q)}$, i.e., one is able to quantify the statistical properties of higher order structure function by knowing the statistics of the structure function of order 3. Note that below the inertial scale (dissipation scale), the linearity is violated.

Empirically, the pertinence of turbulence methods requires in-situ multi-point measurements. In general, satellite observations of the terrestrial plasma environment are single-point time series measurements. In the interplanetary medium for example, satellites such as Wind and ACE are assumed to be nearly at rest with respect to the solar wind motion. In this context, the solar wind velocity and magnetic field measurements constitute data sets that enable to explore the validity of the Magnetohydrodynamic (MHD) approximation, and test plasma turbulence models of a natural system when certain physical conditions are fulfilled. A number of extended studies of solar wind using turbulence have been reported (Carbone et al., 1997; Pagel & Balogh, 2002).

However, one should emphasize that in order to validate such studies one has to identify the limitations imposed by the fundamental assumptions based on single-point time series measurements. These assumptions include homogeneity and stationarity over the time range of interest. Under Taylor's frozen turbulence approximation, the structure function at scale τ identifies an eddy at a scale length $\delta = U_0\tau$, where U_0 is the average speed over the time interval considered. The Taylor approximation allows us to define the structure function of order q as follows:

$$S_q(\tau) = \left\langle \, |U(t+\tau) - U(t)|^q \, \right\rangle \tag{5}$$

where the ensemble average $\langle\rangle$ is now equivalent to a time average, given the assumption of stationarity.

In the ionospheric context, turbulence is often triggered by various plasma instabilities giving rise to electron density fluctuations (Kintner et al., 1982). At low altitude (E-region) where the collisional effects between the ionospheric plasma and the upper neutral atmosphere are important, the two-stream (Farley–Buneman) instability is often excited (Farley, 1963; Buneman, 1963) as the main mechanism for the development of electron density irregularities. In the F-region both the gradient-drift and Kelvin-Helmholtz instabilities occur. Various studies revealed that ionospheric plasma structuring, such as sporadic E-layer or the trailing edge of polar cap patches, result from the gradient-drift and Rayleigh-Taylor instabilities (Sato et al., 1968). Ionospheric turbulence is now well established and the inherent mechanisms are well documented in the literature (Kintner & Seyler, 1985). Several studies investigated the turbulent features related to the ionospheric electric field, electron density and magnetic field at various latitudes (Hamza & St-Maurice, 1993; Dyrud et al., 2008). The non-linear development of plasma irregularities and the energy cascade from large to small scales lead to power spectra of electron density fluctuations that are well fitted by a power law (Mounir et al., 1991). This shape of the power spectral density pinpoints to scale invariance similar to what was developed in fluid turbulence theory. An important consequence of the ionospheric turbulence is its impact on the propagation of radio wave signals emitted by Global Navigation Satellite Systems (GNSS). Our main interest lies in the identification of scaling arguments in the scintillation data that are conformal to the arguments used to characterize ionospheric turbulence. By analogy, we will analyze the time series of the signal amplitude measured, at a single point, by a GNSS receiver assuming conditions similar to those of Kolmogorov turbulence, namely stationarity, homogeneity and isotropy. We will compute the structure functions and study their dependence on time lag τ. In principle, it is assumed that a radio wave front, propagating through a turbulent ionospheric layer, will be significantly altered, and the distortions strongly linked to the presence of electron density irregularities.

The present analysis requires the assumption of stationarity of the scintillation time series. While this condition is difficult to establish, it is reasonable to assume that the recorded signal is locally stationary if the scintillation time interval is measured over a short duration. Previous studies have indicated that the lifetime of large-scale density gradients exceeds several times the time scale for linear growth of the gradient drift instability (Basu et al., 1990). The Taylor hypothesis is now examined in the context related to the study carried out on amplitude scintillation. On the ground, the measured signal results from the propagation of a radio wave as it propagates through a moving ionospheric plasma. The theoretical determination of the scan velocity (V_{eff}, for effective velocity) is a complex problem as it depends upon the satellite motion, the irregularity drift motion as well as the anisotropy of the irregularity with respect to the geomagnetic field. Assuming a model of irregularity in which the electron density variance is distributed according to a spheroid, several authors attempted to estimate V_{eff} (Rino, 1979; Carrano et al., 2016). Under some conditions at low-latitude, Carrano et al. (2016) derived the following approximation for V_{eff}:

$$V_{eff} \sim 1.11 \frac{\sigma_\Phi}{S_4} \rho_F \tag{6}$$

where S_4 and σ_Φ are the amplitude scintillation and phase variation indices, and ρ_F the first Fresnel zone radius with $\rho_F^2 = \frac{z\lambda}{2\pi \cos\theta}$ in which λ is the carrier wavelength, z is the height of the scattering layer and θ the angle between the zenith and the direction of motion of the emitting satellite. For a high elevation angle and assuming the scattering layer is located within the F-region (~ 300 km), the corresponding L-band effective scan velocity $V_{eff} \sim 100 \frac{\sigma_\Phi}{S_4}$. Based on numerous index measurements, it is reasonable to consider that a rule of thumb $\frac{\sigma_\Phi}{S_4} \sim 1-2$ (Ghobadi et al., 2020) yielding an estimation of V_{eff} in the $100-200$ m/s range. In order for the Taylor hypothesis to hold, the scan

speed should remain significantly smaller than the speed of any changes affecting the irregularity. To be more specific, Taylor's hypothesis postulates a linear relationship, non-dispersive, between frequency and wavenumber, $\omega' = \omega + kV_0 \simeq kV_0$, where V_0 is the velocity of the plasma turbulent flow over the detector, ω' (ω) is the measured (plasma rest) frequency. In principle, if one identifies V_0 with V_{eff}, then one would require a large effective velocity for Taylor's hypothesis to remain valid.

Moreover, we assume that the ionospheric turbulence, with a measured power spectrum, is driven by instability mechanisms that allow the development of density structures, which in turn act as random scatterers (Rufenach, 1972). The analogy consists of treating the recorded radio signal by the GNSS receiver as similar to the to single-point measurement of the flow velocity in a turbulent medium that can be modelled using the Kolmogorov (1962) model (Falcon, 2010). Wave turbulence in the terrestrial plasma environment has been addressed theoretically (Sagdeev, 1979) as well as from the observations point of view.

Under the conditions described above, for a time series of the signal amplitude $u(t)$, the turbulence estimator is defined in a similar way as:

$$S_q(\tau) = \left\langle \, |u(t+\tau) - 2u(t) + u(t-\tau)|^q \, \right\rangle \tag{7}$$

where $\langle\rangle$ represents time averages. Note that the expression between bracket is related to the second time derivative of the amplitude $u(t)$ for small lag-times.

$$\frac{d^2u(t)}{dt^2} = \lim_{\tau \to 0} \frac{1}{\tau^2}[u(t+\tau) - 2u(t) + u(t-\tau)] \tag{8}$$

The choice of the structure function expression (7) rather than expression (5), although not fundamental, is justified according to the following argument. The analogy between wave turbulence and fluid turbulence remains limited as the underlying governing equations are different. Fluid turbulence is caused by the presence of viscous forces that lead to relative motions within the fluid. Relative motions can also be produced by the injection of high or low streams inside the fluid. On the other hand, wave turbulence arises from the nonlinear interaction of waves excited through instability mechanisms. Initially of small amplitude, waves excited through instabilities undergo further growth reaching large enough amplitudes to nonlinearly interact with the background flow and other waves within the emitted spectrum; this in turn will lead to saturation if a stationary equilibrium is possible. The nonlinear interaction of waves leads to a distribution of power over spatial and temporal scales that can be modelled, under some important assumptions, by Kolmogorov-like power laws (cascade models). Moreover, one important feature of fluid turbulence is intermittency, which results from bursts of intense motion that are produced and dominated by small scale structures. Therefore, intermittent systems are characterized by non-Gaussian probability density functions imputed to the formation of vortices. In wave turbulence, however, the intermittency is often due to low wave number Fourier amplitude (Choi et al., 2005), not necessarily related to hydrodynamics turbulence. While fluid turbulence is driven by the equation of motion, which involves the first time derivative of U, the wave turbulence is rather governed by the wave equation, which contains the second-time derivative of the wave amplitude. In the former case, the structure function is consistent with Expression (5), while in the latter case, it is conform with Expression (7).

3 Scintillation data

GPS amplitude measurements used in the present study are from the Canadian High Arctic Ionospheric Network (CHAIN) (Jayachandran et al., 2009). With 28 GISTM receivers and 9 ionosondes, the nettwork's coverage expands over Canada northern region.

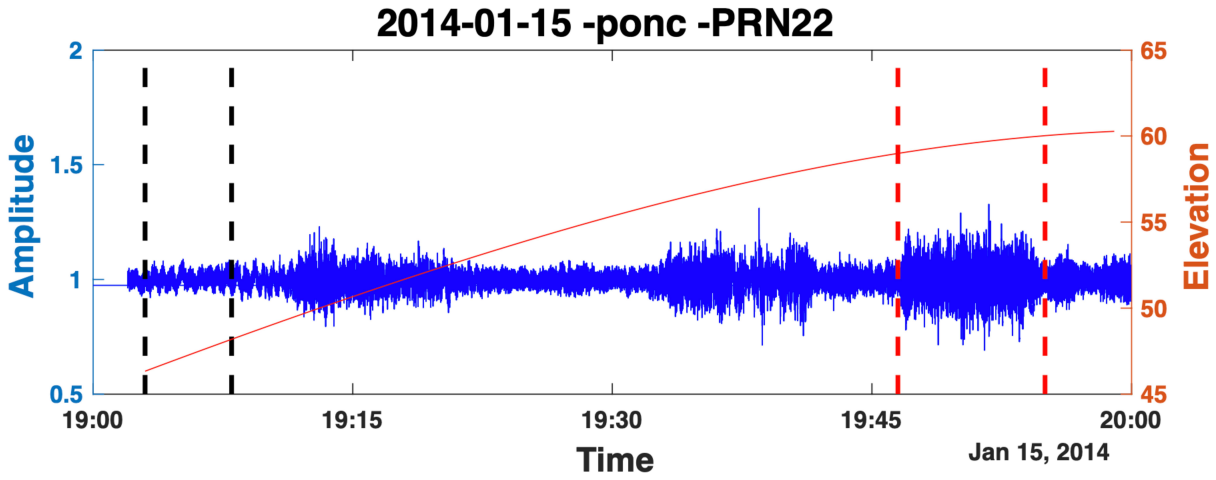

Figure 1. Time series of the amplitude scintillation recorded on January 15, 2014, 1900-2000 UT at *Pond-Inlet* station and from PRN 22. The red continuous line indicates the satellite elevation angle. The red (black) dashed vertical bars mark the time interval of the analyzed event (background).

Data collected by the receivers located at *Pond-Inlet*, (*ponc*) Magnetic Coordinates = (82.3°N, 2.6°E) and *Arctic Bay* (*arcc*) Magnetic Coordinates = (82.1°N, 27.0°E) are of interest in the present work; both stations are located in the statistical cusp region. One should mention that the selection of these 2 stations is not dictated by any physical consideration except by the good quality of data at these stations. Both stations *ponc* and *arcc* operate with high rate GNSS measurements at 50 Hz. In order to eliminate effects due to satellite motion, a detrending operation using a standard sixth order Butterworth filter with a cutoff frequency of $f_c = 0.1$ Hz was applied to the signal prior to any analysis (Mushini, 2012). Given the PRN high elevation angle associated with the events studied below, it is unlikely that these events result from multi-path. In addition, with the same PRNs, no amplitude fluctuations level above the background are noticed prior and after one sidereal day the time of interest. Therefore, the possibility that events analyzed below result from multi-path is ruled out as it is assured that they correspond to scintillation of ionospheric origin.

4 Results

4.1 2014 January 15 event

Figure 1 shows the L1 signal amplitude of PRN number 22 and recorded by a GPS receiver located at *ponc* station on January 15, 2014, 1900 – 2000 UT. The selected interval reveals time segments where amplitude fluctuations are enhanced (1911-1918 UT, 1921-1942 UT, 1946-1955 UT) comparatively to others corresponding to the receiver background level (1903-1908 UT). It is believed that these enhanced fluctuations result from scattering of the radio signal propagating through Fresnel scale ionospheric structures. The continuous red curve indicates the elevation angle of the ray path during the hour. The analysis sequence is now carried out on the time segment marked by the two red vertical bars, i.e. 1946−1955 UT interval where the amplitude fluctuations appear the highest during the hour. In comparison, the two black vertical bars indicate a selected time interval for the receiver background (1903−1908 UT). We mention that the year 2014 corresponds to a near solar maximum activity phase in which ionospheric scintillation occur more frequently (Akala et al., 2011; Meziane et al., 2020). The structure func-

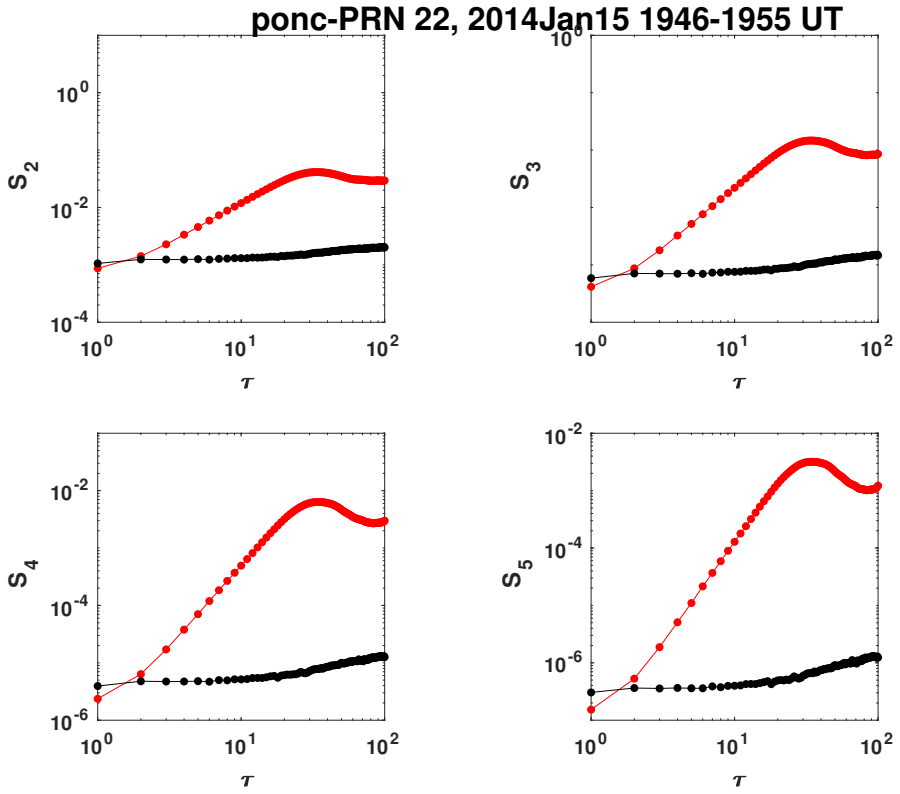

Figure 2. In red, the structure function for $q = 2, 3, 4, 5$ is plotted versus the time scale τ for the time interval 1946 − 1955 UT on 2014 January 15 at *Pond-Inlet* station. The same computation is undertaken in absence of scintillation and the result is represented by the plot in black.

tions of order $q = 1$ to $q = 6$ are now empirically calculated at various time scale τ using scintillation data collected by CHAIN. At this time, we contemplated that no valuable information is gleaned for numerical values of $q > 6$. Figure 2 shows the variation of the structure function S_q (Expression 7) for $q = 2, 3, 4, 5$ versus the time scale τ taken over a continuous interval. A common feature, the shape of the structure function, is revealed for all values of q considered. A similar pattern is obtained for $q = 1$ and $q = 6$ (not shown). While the red plot represents the scintillation event, the back curve corresponds to the receiver background signal for which S_q is also computed. For clarity and in order to display the quantitative feature of S_q for various q, the same $y-$axis limit range is set. Qualitatively, a similar trend appears for all q index values. While S_q for the receiver background signal is found to be nearly independent of the time-scale τ, it exhibits a characteristic signature when ionospheric scintillation is present. In particular, we note that for all values of the q index there exists a range $\Delta\tau$ for which the structure function is linear in τ, $S_q \sim \tau^{\xi(q)}$ (the plots on Figure 2 are in log-log scale). In this particular case, Figure 2 clearly shows that the slope $\xi(q)$ increases with q. In order to precisely identify the range $\Delta\tau$ over which S_q is linear in τ, the derivative of S_q with respect to τ is numerically computed by taking the difference $\Delta S_q(\tau)$ of the structure function between two adjacent points, i.e. $\Delta S_q(\tau) = S_q(\tau + 1) - S_q(\tau)$. Figure 3 shows the obtained results. As shown on this last figure, the variations of $\Delta S_q(\tau)$ displays three distinct ranges. First, a prevailing range where $\Delta S_q(\tau)$ plateaus according to a numerical value that increases with q. A close inspection indicates that this range is established between $\tau = \tau_1 = 3$ and $\tau = \tau_2 = 15$, corresponding to times $t_1 = 0.06s$ and $t_2 = 0.30s$. Below the time scale τ_1, the linearity of the structure function is not

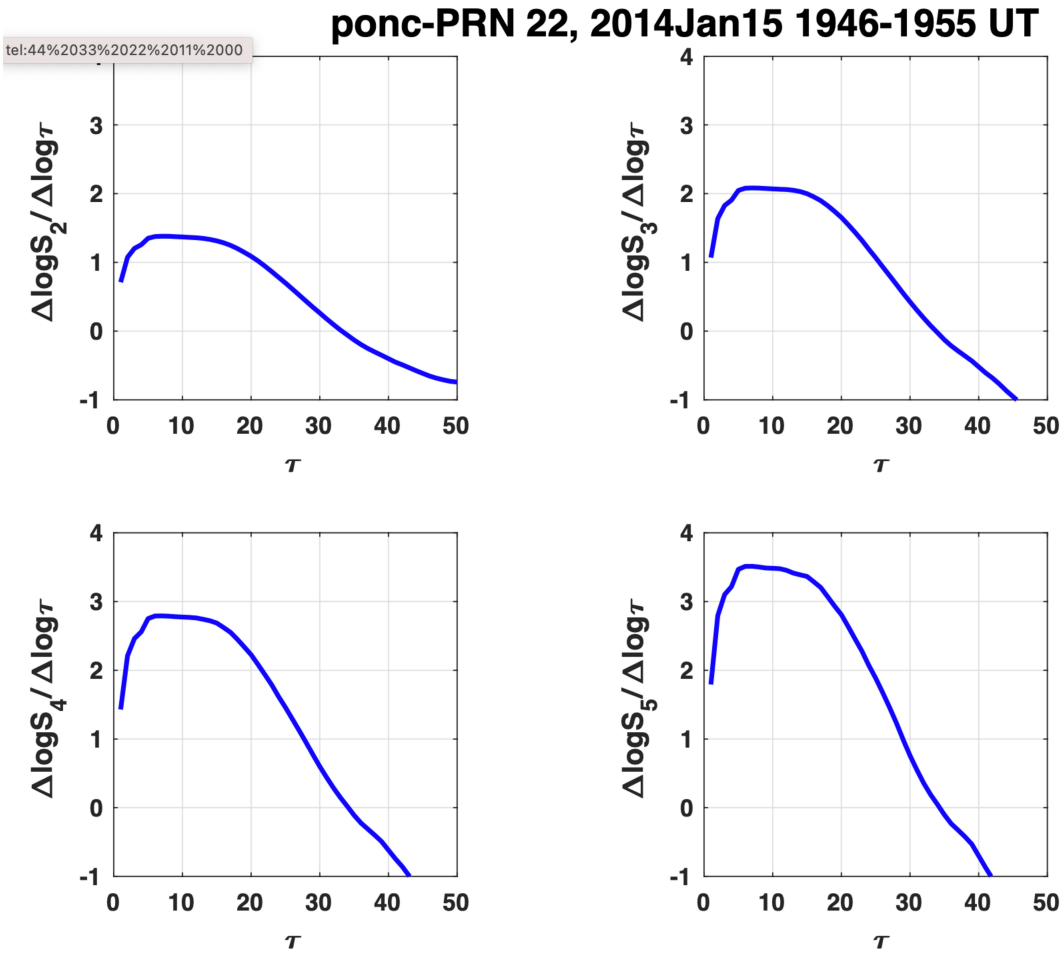

Figure 3. Variation of the difference $\Delta S_q(\tau) = S_q(\tau + 1) - S_q(\tau)$ versus τ for various values of $q-$index.

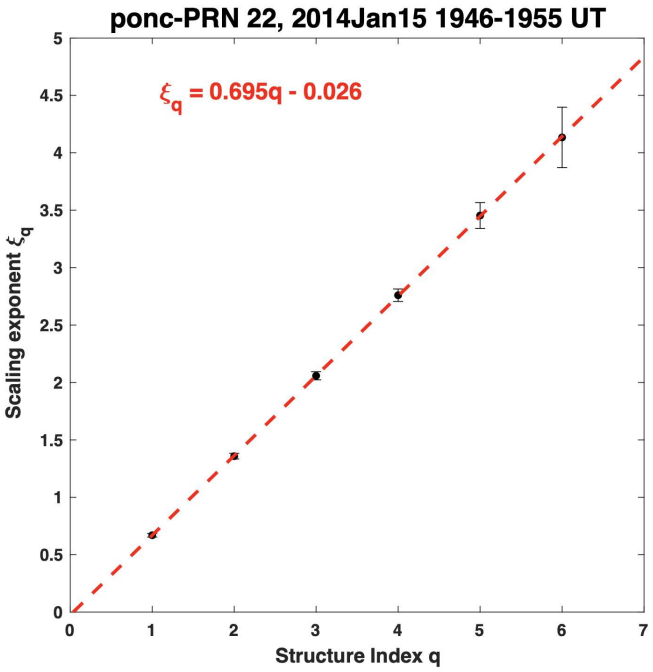

Figure 4. Scaling component ξ_q versus $q-$index within the range. The red dashed line represents the best linear fit.

validated, while for $\tau > \tau_2$ the linearity is broken and the structure function seems to reach a saturation level. To complete the analysis, it is instructive to examine the numerical values for the scaling component $\xi(q)$ in terms of q. The obtained results are shown on Figure 4, which clearly indicate that the scaling component in the range is $\xi(q)/q \approx 0.695$. Further exploration of the shape of the distribution across the time scale τ is examined in the next event.

4.2 2016 October 14 event

The same analysis, as performed above, is now carried out with a second scintillation event recorded at *Arctic Bay* (*arcc*) station on October 14, 2016, in $1723-1728$ UT interval indicated by the two red-dashed vertical bars shown on Figure 5. Also, the two black dashed vertical bars mark the considered receiver background fluctuations level in absence of scintillation ($1732-1742$ UT). The treatment of a supplementary event with similar qualitative result may appear redundant. Nevertheless, the exposition of the event has the purpose to evidence the existence of a linear range in the ionospheric function for ionospheric scintillation.Again, the structure function (Expression 7) as a function of time lag τ is computed for various values of q for both the selected intervals for the scintillation event and the background signal amplitude fluctuations; the result is shown on Figure 6. The presence of a linear range is evident for all values of q shown. A judicious inspection yields an inertial range between $\tau_1 = 30$ and $\tau_2 = 40$ ($0.6 - 0.8$ sec range) with a scaling component $\xi(q)/q \approx 1.1$, significantly higher when compared to the one obtained for the January 17, 2014 event.

The structure function at scale τ examined above is related to the moments of the distribution function of the second order difference in the signal amplitude $\eta(t) = u(t+\tau)-2u(t)+u(t-\tau)$, where $u(t)$ is the scintillation amplitude. The global shape of the distribution density is reflected in the variation of the structure function as exhibited on Figure 2 and Figure 6. The distribution of $\eta(t)$ across the scales for few selected increas-

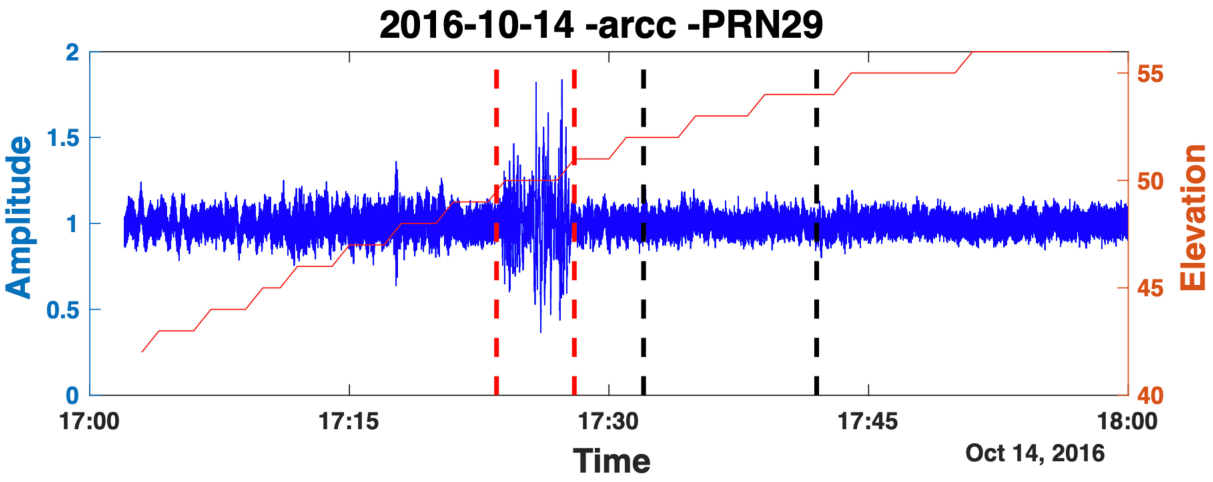

Figure 5. Time series of the amplitude scintillation recorded on October 14, 2016, 1700-1800 UT at *Arctic Bay* station and from PRN 29. The red continuous line indicates the satellite elevation angle. The red (black) dashed vertical bars mark the time interval of the analyzed event (background).

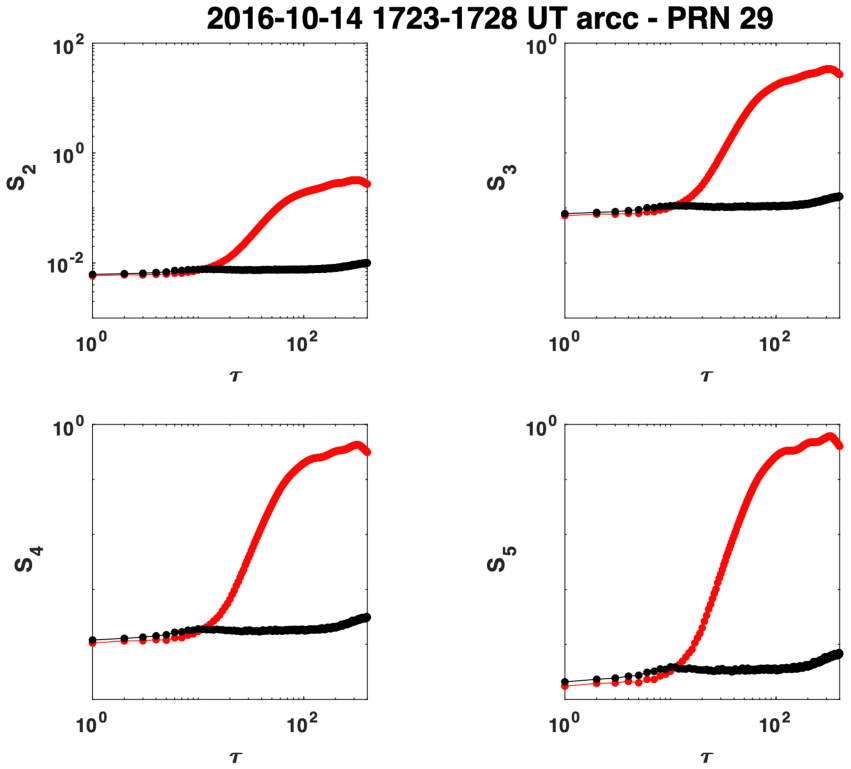

Figure 6. In red, the structure function for $q = 2, 3, 4, 5$ is plotted versus the time scale τ for the time interval $1732 - 1728$ UT on 2016 October 14 at *Arctic Bay* station. The same computation is undertaken for the receiver background signal and the result is represented in black in the various plots.

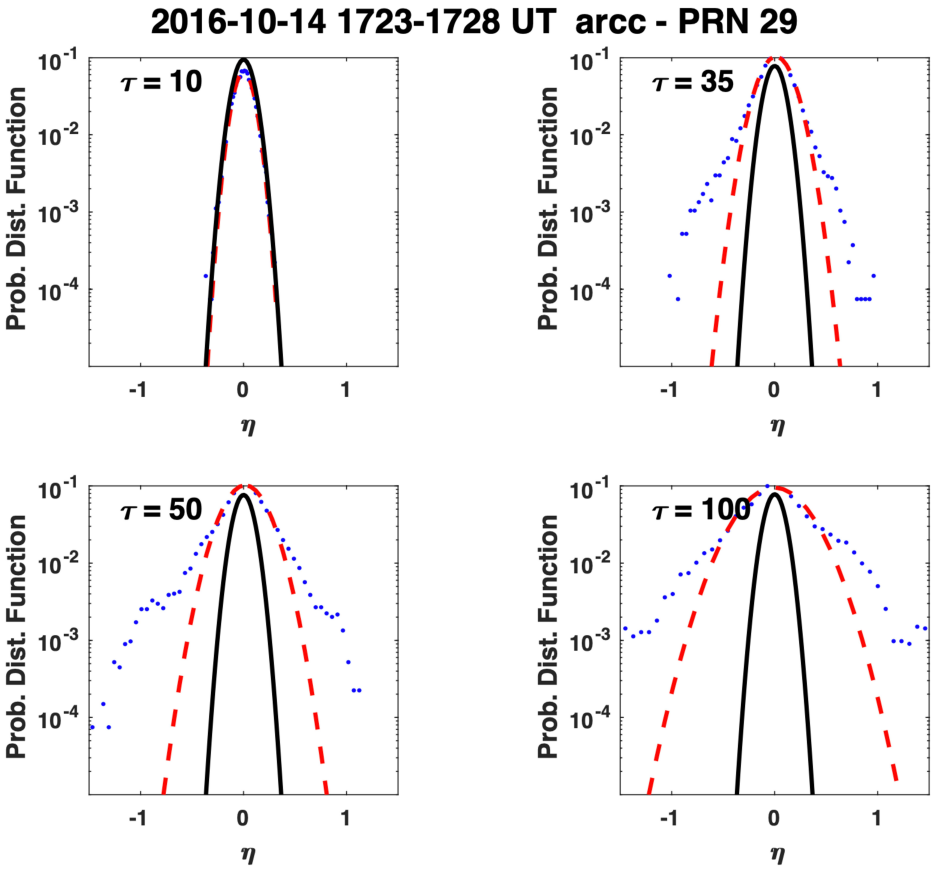

Figure 7. The blue dots represent the measured probability distribution function of $\eta(t)$ for time lags $\tau = 10, 35, 50, 100$ associated with the event interval indicated by the figure title. The red-dashed line corresponds to the best Gaussian fit to the measurement while the black continuous curve shows the distribution when no scintillation is present (background).

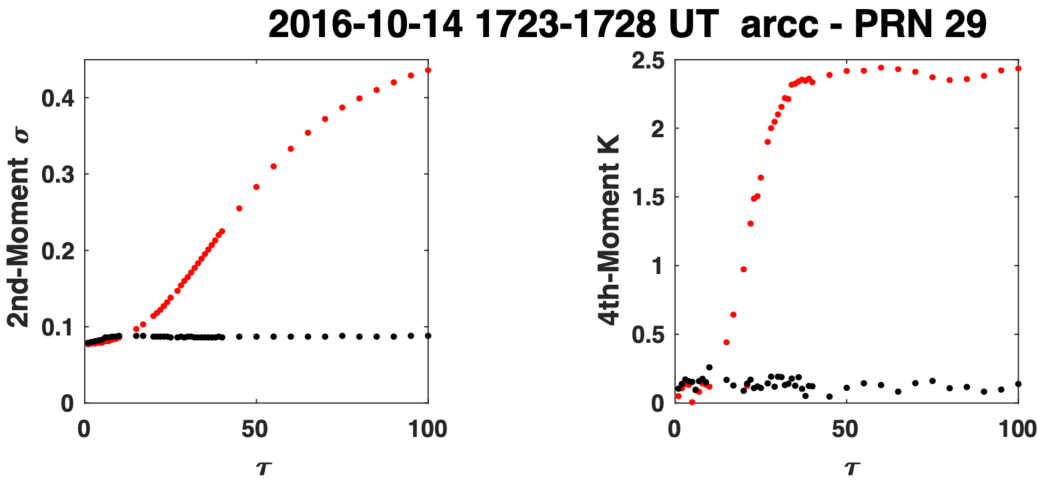

Figure 8. Second moment of distribution (left panel) and excess kurtosis (right panel) of $\eta(t)$ versus the time lag τ. The red dots correspond to the scintillation event while the black dots represent the background noise.

ing values of τ is shown on Figure 7. While the measurements are represented by the blue marks, the dashed red line corresponds the best Gaussian fit to the data. At the same time, the probability density of $\eta(t)$ fluctuations in the absence of scintillation is given by the continuous black curve. Clearly, the receiver background probability density remains invariant, while in the case of scintillation event the distribution undergoes a continuous widening departing from the Gaussian shape at higher scales. The peak of the distribution is satisfactorily fit using a Gaussian, but the emerging tails with increasing scale τ cannot be captured with Gaussian statistics. Departures from Gaussian statistics are usually quantified by distribution moments with orders higher than 2. In particular, the relevance of the tail is captured by the excess kurtosis (= 0 for a Gaussian). Panels on Figure 8 show the computed second (left panel) and forth moments (right panel) of $\eta(t)$ for increasing scale τ, respectively. The red (black) marks correspond to numerical values obtained for the scintillation event (receiver background). Clearly, for the background signal, the computed moments appear insensitive to changes of τ and the excess kurtosis remains near a zero value as it is expected of a Gaussian process. On the contrary, for the scintillation event both moments increase with τ before reaching an asymptotic limit ($K \approx 2.4$). It is remarkable that the kurtosis K attains the asymptotic value at $\tau \approx 40$, basically the upper bound of the linear range.

5 Discussion and Conclusion

Analysis methods developed in the context of neutral fluid and plasma turbulence theory are adopted to explore the pertinent spatio-temporal scales in ionospheric scintillation physics. A justification of the approach is based on the consideration that ionospheric scintillation is produced when the radio signal propagates through a non-homogeneous medium undergoing at the same time spatio-temporal fluctuations. We have computed the structure function of order q, defined in our case as a second order difference in the signal amplitude at temporal scale τ is computed for various orders q. Qualitatively and through the perspective of fluid turbulence, the resulting variations of S_q as a function of τ are analogous to the numerical findings in Navier-Stokes turbulence (Benzi et al., 1993; Grossmann et al., 1997), wave turbulence (Falcon, 2010), and empirical results such those related to the solar wind turbulence (Carbone et al., 1997; Pagel & Balogh, 2002; Weygand et al., 2006). From the variations of S_q emerges a linear range analog to the

inertial range of fluid turbulence. Below the linear range, the linearity of the the structure function is not satisfied, which seems to pinpoint to a dissipation range counterpart. The obtained scaling component value, which is event-dependent, is larger than the value found in Kolmogorov's turbulence ($\xi_3 > \xi_3^{(Kol)} = 1$). The essence of our study of higher order structure functions is to try and identify patterns in their behaviours with time delay like those found in the first, second and third order structure functions. The recurrent linear behaviour with time delay is present in all the structure functions studied up to order 6. As mentioned above, the relationship $S_q \sim S_3^{\xi(q)}$ explains this characteristic (when considering the log of the structure functions). Within the ionospheric plasma, the structure function has been previously constructed by means of numerical simulations and in-situ measurement in order to unveil the precise scaling features related to ionospheric turbulence. Specifically, the electrostatic potential in the E-region (Dyrud et al., 2008) and electron density at the topside F-layer (De Michelis et al., 2021) provide the pertinent physical quantities for the analysis. For the electrostatic fluctuations, the structure functions for various q, and captured at a fixed point, increase with time lag and exhibit a linear range. At the same time, the probability density for the potential fluctuations follow a nearly Gaussian distribution. Furthermore, the numerical values obtained for the scaling exponents, when compared to those derived from rocket data based on two-point measurements, appear noticeably smaller (Dyrud et al., 2008). Nevertheless, the empirical determination of the scaling component appear similar to the scintillation equivalent linear range in the case $q = 1 - 4$. More recently, in a study reported by De Michelis et al. (2021), the scale invariance associated with ionospheric electron density fluctuations has been empirically investigated. The authors used in-situ 1 Hz rate electron density measurements from the ESA-Swarm A satellite to evidence the existence of an inertial scale range associated with the plasma turbulence at the topside ionosphere. In the cusp region, De Michelis et al. (2021) found that the first-order ($q = 1$) scaling exponent numerical value is comparable to the one obtained from the scintillation data analyzed in the present study. This concordance strongly indicates that the scaling features present in the ionospheric electron density fluctuations coherently echo in scintillation seen on the ground. Particularly, scintillation may possibly be considered as a proxy for ionospheric turbulence. The extension of the present study to a larger collection of scintillation events could precise this aspect. Below the linear range, it is found that the structure function increases with time lag τ, a feature similar found in wave turbulence theory. In fluid turbulence, the dissipation region is dominated by enhanced fluctuations of short durations. This feature, commonly called intermittency, is also observed in wave turbulence. A scrutiny of the distribution function of fluctuations of the variable of interest in the intermittent region exhibits strong departure from the conventional Gaussian statistics. While the distribution function remains nearly symmetric (skewness ~ 0), it reveals at the same time pronounced tails of flatness with a positive residual kurtosis (leptokurtic distribution). The bending of the structure function, when the time scale τ is larger than the linear range, suggests that amplitudes in the signal separated by a long time-lag tend to be uncorrelated; no long time memory. One therefore expects Gaussian statistics for long-time scales. In other words, while all odd moments of the distribution of $\eta(t)$ vanish, the standardized even moments have fixed numerical values independent of the variance. Particularly, the excess kurtosis (fourth moment distribution) at large τ is close to zero. These results have been established theoretically and empirically for both fluid and wave turbulence (Falcon, 2010), respectively. This picture is associated with diffusion processes and derived from the solutions of Fokker-Planck or Langevin equations.

The results reported in the present work seemingly contrast with the prediction of a Gaussian closure as indicated by the non-zero asymptotic value of the residual kurtosis. The scattered radio signal through the ionosphere seems to be related to processes that are not fully uncorrelated over a range of length scales. A random-walk interpretation of the results suggests a wave-scattering process leading to non-Gaussian signa-

tures that arise when the steps of the walker happen to be correlated in a hierarchical way. Therefore, a proper and adequate understanding of the reported results, which need to be extended to include a larger data base in addition to a parametric study, requires the adoption of non-Gaussian models. A possible solution consists of exploring the scaling exponent for various geomagnetic conditions, and its latitude-dependence as well as an eventual association with the amplitude index S_4. Such non-Gaussian models, among others, that are related to wave propagation through non-homogeneous media have been previously highlighted (Jakeman & Tough, 1988). In this respect, a model based on K-distribution that describes the amplitude of scattered waves through a rough surface seems to have attractive features as it provides practical statistical properties that could be examined within the ionosphere context. Indeed, drawing a parallel between a structured ionospheric layer and an object with a rough surface can be very instructive when one considers the scattering of a radio wave by the ionosphere and the scattering of light by a rough surface. The emerging pattern from laser scattering by a rough surface is analogous to the scintillation pattern observed when a radio wave propagates through a structured ionosphere dominated by Fresnel-size scatterers. The analogy suggests a strong role played by diffraction in the production of ionospheric scintillation (McCaffrey & Jayachandran, 2019). This path of studying the scintillation pattern though the lens of the diffraction by a rough object surface lies beyond the scope of our investigation.

Acknowledgments

CHAIN data are available through http://www.chain-project.net/data/gps/data/raw/ponc/2014/01/ website. Infrastructure funding for CHAIN was provided by the Canadian Foundation for Innovation and the New Brunswick Innovation Foundation. CHAIN operations are conducted in collaboration with the Canadian Space Agency. This research was undertaken with the financial support of the Canadian Space Agency FAST program and the Natural Sciences and Engineering Research Council of Canada.

References

Aarons, J. (1982). Global morphology of ionospheric scintillations. *IEEE Proceedings*, *35*, 360—378.

Akala, A. O., Doherty, P. H., Valladares, C. E., Carrano, C. S., & Sheehan, R. (2011). Statistics of GPS scintillations over south america at three levels of solar activity. *Radio Sci.*, *46*, RS5018. doi: 10.1029/2011RS004678

Basu, S., Basu, S., MacKenzie, R., Coley, W. R., Sharber, J. R., & Hoegy, W. R. (1990). Plasma structuring by the gradient drift instability at high latitudes and comparison with velocity shear driven processes. *J. Geophys. Res.*, *95*, 7799-7818.

Benzi, R., Ciliberto, S., Tripiccione, R., Baudet, C., Massaioli, F., & Succi, S. (1993). Extended self-similarity in turbulent flows. *Phys. Rev. E*, *48*, 29–32.

Buneman, O. (1963). Excitation of field aligned sound waves by electron streams. *Phys. Rev. Lett.*, *10*, 285.

Carbone, E., Bruno, R., & Veltri, P. (1997). Evidences for extended self-similarity in hydromagnetic turbulence. *Geophys. Res. Lett.*, *23*, 121–124.

Carrano, C. S., Groves, K. M., Rino, C. L., & Doherty, P. H. (2016). A technique for inferring zonal irregularity drift from single stationgnss measurements of intensity (S_4) and phase (σ_Φ) scintillations. *Radio Sci.*, *51*, 1263–1277. doi: 10.1002/2015RS005864

Chang, T. T. S. (2015). Probability distribution and structure functions. In *An introduction to space plasma complexity* (pp. 75–88). Cambridge University Press. Retrieved from `https://doi.org/10.1017/CBO9780511980251` doi: 10.1017/CBO9780511980251

Choi, Y., Lvov, Y. V., Nazarenko, S., & Pokorni, B. (2005). Anomalous probability of large amplitudes in wave turbulence. *Phys. Lett. A*, *339*, 361–369.

De Michelis, P., Consolini, G., Pignalberi, A., Tozzi, R., Coco, I., Giannattasio, F., ... Balasis, G. (2021). Looking for a proxy of the ionospheric turbulence with swarm data. *Nature Scientific Reports*, *11*, 6183. Retrieved from https://doi.org/10.1038/s41598-021-84985-1 doi: 10.1038/s41598-021-84985-1

Dyrud, L., Krane, B., Oppenheim, M., Pécseli, H. L., Trulsen, J., & Wernik, A. W. (2008). Structure functions and intermittency in ionospheric plasma turbulence. *Nonlin. Processes Geophys.*, *15*, 847—862. Retrieved from www.nonlin-processes-geophys.net/15/847/2008/

Falcon, E. (2010). Laboratory experiments on wave turbulence. *Discrete and Continuous Dynamical Systems, Series B*, *13*, 919–940. doi: 10.3934/dcdsb.2010.13.819

Farley, D. T. (1963). Two-stream plasma instability as a source of irregularities in the ionosphere. *Phys. Rev. Lett.*, *10*, 279.

Ghobadi, H., Spogli, L., Alfonsi, L., Cesaroni, C., Cicone, A., Linty, N., ... Cafaro, M. (2020). Disentangling ionospheric refraction and diffraction effects in gnss raw phase through fast iterative filtering technique. *GPS Solut.*, *24*, 85. Retrieved from https://doi.org/10.1007/s10291-020-01001-1 doi: 10.1007/s10291-020-01001-1

Grossmann, A., Lohse, D., & Reeh, H. (1997). Application of extended self-similarity in turbulence. *Phys. Rev. E*, *56*, 5413–5478.

Groves, K. M., Basu, S., Weber, E. J., Smitham, M., Kuenzler, H., Valladares, C. E., ... Kend, M. J. (1997). Equatorial scintillation and systems support. *Radio Sci.*, *32*, 2047–2064.

Hamza, A. M., & St-Maurice, J.-P. (1993). A turbulent theoretical framework for the study of current-driven E region irregularities at high latitudes: Basic derivation and application to gradient-free situations. *J. Geophys. Res.*, *98*, 11,587–11,599.

Jakeman, E., & Tough, R. J. A. (1988). Non-Gaussian models for the statistics of scattered waves. *Adv. in Physics*, *37*, 471–529.

Jayachandran, P. T., Langley, R. B., MacDougall, J. W., Mushini, S. C., Pokhotelov, D., Hamza, A. M., ... Carrano, C. S. (2009). Canadian High Arctic Ionospheric Network (CHAIN). *Radio Sci.*, *44*, RS0A03. doi: 10.1029/2008RS004046

Kintner, P. M., Kil, H., Beach, T. L., & de Paula, E. R. (2001). Fading timescales associated with GPS signals and potential consequences. *Radio Sci.*, *36*, 731–743.

Kintner, P. M., Ledvina, B. M., & de Paula, E. R. (1982). Non-linear evolution of plasma enhancements in the auroral ionosphere, 1. Long wavelength irregularities. *J. Geophys. Res.*, *87*, 144-150. Retrieved from https://doi.org/10.1029/JA087iA01p00144 doi: 10.1029/JA087iA01p00144

Kintner, P. M., Ledvina, B. M., & de Paula, E. R. (2007). GPS and ionospheric scintillations. *Space Weather*, *5*, S09003. Retrieved from https://doi.org/10.1029/2006sw000260 doi: 10.1029/2006sw000260

Kintner, P. M., & Seyler, C. E. (1985). The status of observations and theory of high latitude ionospheric and magnetospheric plasma turbulence. *Space Sci. Rev*, *41*, 1572—1672.

Lawrance, A. J. (1991). Directionality and reversibility in time series. *International Statistical Review*, *59*, 67–79. Retrieved from https://www.jstor.org/stable/1403575

McCaffrey, A. M., & Jayachandran, P. T. (2019). Determination of the refractive contribution to gps phase "scintillation". *J. Geophys. Res.*, *124*, 1454—1469. Retrieved from https://doi.org/10.1029/2018JA025759

Mezaoui, H., Hamza, A. M., & Jayachandran, P. T. (2015). High-latitude intermittent ionospheric scintillations: Exploring the castaing distribution. *J. Geophys. Res.*, *120*, 6831–6836. doi: 10.1002/2015JA021304

Meziane, K., Kashcheyev, A., Patra, S., Jayachandran, P. T., & Hamza, A. M. (2020). Solar cycle variations of gps amplitude scintillation for the polar region. *Space Weather*, *18*. Retrieved from `https://doi.org/10.1029/2019SW002434` doi: 10.1029/2019SW002434

Mounir, H., Cerisier, J., Berthelier, A., Lagoutte, D., & Begin, C. (1991). The small-scale turbulent structure of the high-latitude ionosphere arcad-aureol-3 observations. *Ann. Geophys.*, *9*, 725–737.

Mushini, S. C. (2012). *Charcateristics of scintillating gps signal at high-latitudes during solar minima* (Unpublished doctoral dissertation). University of New Brunswick, New Brunswick.

Pagel, C., & Balogh, A. (2002). ntermittency in the solar wind: A comparison between solar minimum and maximum using ulysses data. *J. Geophys. Res.*, *107*, 1178–1185. doi: 10.1029/2002JA009331

Priyadarshi, S. (2015). A review of ionospheric scintillation models. *Surv. Geophysics*, *36*, 295–324. doi: 10.1007/s10712-015-9319-1

Rino, C. L. (1979). A power law phase screen model for ionospheric scintillation, 1. weak scatter. *Radio Sci.*, *14*, 81135-1145.

Rufenach, C. L. (1972). Power-law wavenumber spectrum deduced from ionospheric scintillation observations. *J. Geophys. Res.*, *77*, 4761–4772. doi: 10.1029/JA077i025p04761

Sagdeev, R. Z. (1979). The 1976 Oppenheimer lectures: Critical problems in plasma astrophysics, i. turbulence and nonlinear waves. *Rev. Mod. Phys.*, *51*, 1–9.

Sato, T., Takao, T., & Maeda, K. (1968). Fully developed turbulent irregularities in the ionosphere due to cross-field plasma instability. *Radio Sci.*, *3*, 529—534.

Sosa-Correa, P., Pereira, R. M., Macêdo, A. M. S., Raposo, E. P., Salazar, D. S. P., & Vasconcelos, G. L. (2019). Emergence of skewed non-gaussian distributions of velocity increments in isotropic turbulence. *Phys. Rev. Fluids*, *4*, 064602.

Taylor, G. I. (1935). Statistical theory of turbulence. In *Proc. R. Soc. Lond., A* (pp. 421–444). doi: 10.1098/rspa.1935.0158

Taylor, G. I. (1938). The spectrum of turbulence. In *Proc. R. Soc. Lond., A* (pp. 476–490). doi: 10.1098/rspa.1938.0032

Wernik, A. W., Alfonsi, L., & Materassi, M. (2007). Scintillation modelling using in situ data. *Radio Sci.*, *42*, RS1002. Retrieved from `https://doi.org/10.1029/2006RS003512` doi: 10.1029/2006RS003512

Weygand, J. M., Kivelson, M. G., Khurana, K. K., Schwarzl, H. K., Walker, R. J., Balogh, A., ... Goldstein, M. L. (2006). Non-self-similar scaling of plasma sheet and solar wind probability distribution functions of magnetic field fluctuations. *J. Geophys. Res.*, *111*. doi: 10.1029/2006JA011820

Yeh, K. C., & Liu, C.-H. (1982). Radio wave scintillation in the ionosphere. In *Proceedings of the IEEE* (pp. 324–360).